

A Neural Network-Based Controller for DC-DC Buck Converter for Improved Resilience

Original

A Neural Network-Based Controller for DC-DC Buck Converter for Improved Resilience / Nikiforos, L., Gabriele, F., Prono, L., Pareschi, F., Setti, G.. - STAMPA. - (2025), pp. 1-4. (20th International Conference on PhD Research in Microelectronics and Electronics, PRIME 2025 Taormina (Ita) 21-24 September 2025)
[10.1109/prime66228.2025.11203368].

Availability:

This version is available at: 11583/3005595 since: 2025-12-02T14:36:02Z

Publisher:

Institute of Electrical and Electronics Engineers Inc.

Published

DOI:10.1109/prime66228.2025.11203368

Terms of use:

This article is made available under terms and conditions as specified in the corresponding bibliographic description in the repository

Publisher copyright

IEEE postprint/Author's Accepted Manuscript

©2025 IEEE. Personal use of this material is permitted. Permission from IEEE must be obtained for all other uses, in any current or future media, including reprinting/republishing this material for advertising or promotional purposes, creating new collecting works, for resale or lists, or reuse of any copyrighted component of this work in other works.

(Article begins on next page)

A Neural Network-Based Controller for DC-DC Buck Converter for Improved Resilience

Lorenzo Nikiforos^{*}, Francesco Gabriele^{*}, Luciano Prono^{*}, Fabio Pareschi^{*,†}, Gianluca Setti[‡]

^{*} DET – Politecnico of Torino, corso Duca degli Abruzzi 24, 10129 Torino, Italy.

email: {lorenzo.nikiforos, francesco.gabriele, luciano.prono, fabio.pareschi}@polito.it

[†] ARCES – University of Bologna, via Toffano 2/2, 40125 Bologna, Italy.

[‡] CEMSE, King Abdullah University of Science and Technology (KAUST), Saudi Arabia. email: gianluca.setti@kaust.edu.sa

Abstract—This paper presents a novel Neural Network (NN) based control strategy for DC-DC Buck converters aiming to enhance the dynamic system response in face of external disturbances. The proposed controller employs a compact multilayer perceptron, and it is trained online through supervised learning strategy. Its ground-truth labels correspond to the optimal control actions that minimize the converter output voltage error. This results in a tiny NN, paving the way for embedded hardware implementations. The validation of the proposed NN-based controller is conducted via circuitual simulations, demonstrating significant improvements in transient response compared to conventional control techniques.

Index Terms—DC-DC converters, Neural Network, Tiny Machine Learning, Artificial Intelligence, Gradient Descent.

I. INTRODUCTION

DC-DC converters are ubiquitous elements in modern Cyber-Physical System (CPS) power applications such as DC microgrids, e-mobility, renewable energy systems and IoT. Indeed, since constitute the physical layer of the CPSs, their design need to be conceived including external connectivity features. The latter enable remote monitoring, diagnostics and control of the converter operating setpoints [1]. This provides significant operational advantages and improve the system flexibility [2]. Nonetheless, it increases the vulnerability of the converters to cyber-attacks [3]. Therefore, the introduction of prevention mechanism that ensure the cyber-physical security of these systems is essential.

Several studies focus on the threats posed by cyber-attacks in the field of DC-DC converter. These includes false data injection, denial-of-service, and controller hijacking [4]. The cyber-attacks lead to degraded performance, instability, or even physical damage. Mitigation strategies include anomaly detection algorithms at the control input/output interface, secure communication protocols, and redundant sensing architectures. Among the others, Neural Networks (NNs) offer promising approaches to integrate cyber-attack detection mechanisms owing to their feature extraction capacity [5] [6].

Beyond cyber-security application, NN-based architectures emerged as a flexible and data-driven control approach in DC-DC converters. Rejecting external disturbances and guaranteeing system stability is crucial, as the proper operation of the supplied devices strongly relies on a stable voltage level. NN-based controllers are developed exploiting different approaches such as supervised learning [7] [8] reinforcement learning [9] [10], and physics informed neural networks [11].

In recent works, hybrid NNs co-hosting both control and risks detection features have been proposed [11] [12]. In light of the requirements on the computational time set in power electronic applications, Tiny Machine Learning is necessary. In fact, lightweight NN models are designed to run inference in real time on low-resource hardware platforms [13]. This work is situated precisely within this

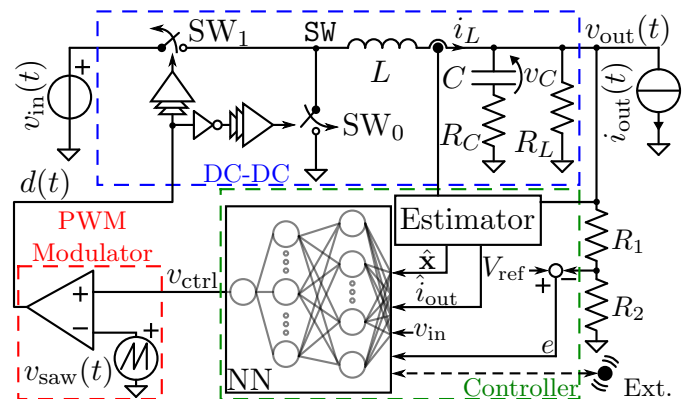


Fig. 1. The DC-DC Buck converter and the proposed NN-based controller.

context, where a small-sized NN is present in the converter and used to improve its resilience, intended both as possible resistance to a cyber-security attack, and as mitigation of a change in the converter parameter set.

In detail, we focus on the part of the tiny NN used for controlling the DC-DC Buck converter. It is derived via a novel online training algorithm that relies on supervised learning. The network is trained to reproduce the optimal control actions in face of external disturbances (e.g., load and line fluctuations). Owing to its structure, the controller can naturally be extended to include cyber-attack detection mechanisms.

The paper is organized as follows. Sec. II introduces the theoretical framework for modeling converter dynamics. Sec. III details the proposed training algorithm, while Sec. IV presents the simulation results. Finally, the conclusions are outlined.

II. ARCHITECTURAL DESCRIPTION AND THEORETICAL BACKGROUND

The DC-DC Buck converter architecture we refer is shown in Fig. 1. The input voltage $v_{in}(t)$ is chopped by the action of the switches $SW_{0,1}$. These are complementary driven by the logic signal $d(t)$, i.e., when $d = 0$ the SW_0 is closed while SW_1 is open, and vice versa for $d = 1$. This results in a rectangular voltage waveform on the SW node $v_{SW}(t)$, that is in turn smoothed-out by the converter output filter. The latter is designed to generate a stable voltage $v_{out}(t)$ on the converter output port and it includes the inductance L , the output capacitor C together with its series parasitic resistance R_C and the resistive load R_L . An additional time-varying load current $i_{out}(t)$ is connected to the converter output port, modeling externally imposed load variations. The signal $d(t)$ is generated from a Pulse-

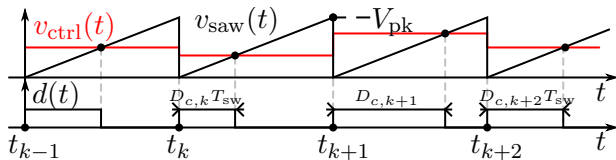


Fig. 2. Waveforms showing the operation of the PWM Modulator in Fig. 1.

Width Modulator (PWM) stage. In this scenario, we will refer to the traditional sawtooth-based PWM [14]. It tunes the duty cycle D_c of the signal $d(t)$ by comparing the control voltage $v_{ctrl}(t)$ and a sawtooth waveform $v_{saw}(t)$ with amplitude V_{pk} . The latter oscillates at a fixed frequency $f_{sw} = 1/T_{sw}$. A representative set of time-domain waveforms illustrating the modulator operation at is shown in Fig. 2.

The Buck converter operation can be described resorting to its state-space representation [14]. In the following, we will denote matrices with boldface capital letters (e.g., \mathbf{V}) and vectors with boldface lowercase letters (e.g., \mathbf{v}). Referring to Fig. 1, the independent states of the system are defined by the vector $\mathbf{x}(t) = [i_L(t), v_C(t)]^T$, while its independent inputs are $\mathbf{u}(t) = [v_{in}(t)d(t), i_{out}(t)]^T$, where T denotes the transpose operator. We consider the converter output voltage as the system output, i.e., $y(t) = v_{out}(t)$. Therefore, straightforward circuit analysis yields

$$\begin{aligned} \dot{\mathbf{x}}(t) &= \mathbf{A}\mathbf{x}(t) + \mathbf{B}_\gamma\mathbf{u}(t) \\ \mathbf{y}(t) &= \mathbf{C}\mathbf{x}(t) + \mathbf{D}\mathbf{u}(t), \end{aligned} \quad (1)$$

where \mathbf{A} , \mathbf{B}_γ , \mathbf{C} and \mathbf{D} denote the state, input, output, and feedforward matrices, respectively. Their analytical expressions for the circuit in Fig.1 are detailed in Table I. The parameter γ takes on the logic state of d .

The time-domain evolution of the converter is derived solving the state-space equations in (1). Referring to the generic k^{th} switching period shown in Fig. 2, i.e., $t \in [t_k, t_{k+1}]$, we aim to evaluate $\mathbf{x}(t_{k+1})$ from $\mathbf{x}(t_k)$. Since the signal $d(t)$ is piece-wise linear, we will separately evaluate the system evolution in the time intervals $[t_k, t_k + D_{c,k}T_{sw}]$ and $[t_k + D_{c,k}T_{sw}, t_{k+1}]$, corresponding to $d = 1$ and $d = 0$, respectively. Furthermore, it is reasonable to consider the system inputs $\mathbf{u}(\tau)$ as constants in each switching cycle [15]. In other words, we consider $\mathbf{u}(\tau) = \mathbf{u}(t_k)$ in the k^{th} switching period. This lead to the sampled-data system description:

$$\begin{aligned} \mathbf{x}(t_{k+1}) &= e^{\mathbf{A}T_{sw}}\mathbf{x}(t_k) + \mathbf{A}^{-1} \left(\left[e^{\mathbf{A}T_{sw}} - e^{\mathbf{A}(1-D_{c,k})T_{sw}} \right] \mathbf{B}_0 \right. \\ &\quad \left. + \left[e^{\mathbf{A}(1-D_{c,k})T_{sw}} - \mathbf{I} \right] \mathbf{B}_1 \right) \mathbf{u}(t_k), \\ \mathbf{y}(t_k) &= \mathbf{C}\mathbf{x}(t_k) + \mathbf{D}\mathbf{u}(t_k). \end{aligned} \quad (2)$$

As shown in Fig. 1, the value of $D_{c,k}$ is set from the PWM stage based on the v_{ctrl} in the k^{th} switching cycle, namely, $D_{c,k} = v_{ctrl}(t_k + D_{c,k}T_{sw})/V_{pk}$. The controller stage processes the input signals i_L and v_{out} to produce v_{ctrl} . It embeds the proposed NN and the Estimator stage [16] [17]. The latter gives an estimate of the system states and the load current disturbance, here denoted as \hat{x} and \hat{i}_{out} , respectively. These signals are provided as inputs to the NN, together with v_{in} and the error signal $e = V_{ref} - R_2/(R_1 + R_2)v_{out}$. The resistances $R_{1,2}$ are chosen so that $V_{out}^{target}(1 + R_1/R_2)$, where V_{out}^{target} is the target output voltage value. It is worth noting that, in contrast to v_{in} , the \hat{i}_{out} can be only estimated as it is not a directly measurable signal.

TABLE I
 STATE-SPACE MATRICES OF THE BUCK CONVERTER SHOWN IN FIG. 1.

$\mathbf{A} = \begin{pmatrix} -\frac{(R_C R_L)}{L} & -\frac{R_L}{L(R_C+R_L)} \\ \frac{R_L}{C(R_L+R_C)} & -\frac{1}{C(R_L+R_C)} \end{pmatrix}$	$\mathbf{B}_\gamma = \begin{pmatrix} \frac{(1-\gamma)}{L} & \frac{(R_C R_L)}{L} \\ 0 & -\frac{R_L}{C(R_L+R_C)} \end{pmatrix}$
$\mathbf{C} = \begin{pmatrix} R_C R_L & \frac{R_L}{R_C R_L} \end{pmatrix}$	$\mathbf{D} = \begin{pmatrix} 0 & -R_C R_L \end{pmatrix}$

III. PROPOSED TRAINING OF THE NEURAL NETWORK

A custom training strategy is developed for the NN-based controller. It is an online supervised learning strategy based on the optimal $D_{c,k}$ minimizing e under varying operating conditions of the converter.

A. Duty-Cycle Optimization Method

From (2), the optimal $D_{c,k}$ is computed minimizing a cost function J_k penalizing large e values. This is accomplished further ensuring that meaningful $D_{c,k}$ values are derived. In formulas

$$\begin{aligned} \min_{D_{c,k}} J_k &\stackrel{\text{def}}{=} e^2(t_k) \\ \text{subject to} & \quad 0 \leq D_{c,k} \leq 1. \end{aligned} \quad (3)$$

This corresponds to a constrained optimization task that is solved via an iterative projected gradient descent algorithm. In the iteration step i , the $D_{c,k}^{(i)}$ is updated by moving in the direction opposite to the gradient of J_k and clipped in the range $[0, 1]$ in order to satisfy the constraint. Then, the $D_{c,k}^{(i)}$ is updated to $D_{c,k}^{(i+1)}$ as

$$D_{c,k}^{(i+1)} = \min \left\{ 1, \max \left(0, D_{c,k}^{(i)} - \alpha \frac{\partial J_k}{\partial D_{c,k}} \Big|_{D_{c,k}^{(i)}} \right) \right\}, \quad (4)$$

where $\alpha > 0$ is the step-size. By repeating the optimization process until no improvements in minimizing J_k are detected, the optimal $D_{c,k}$ is derived, here denoted as $D_{c,k}^*$.

B. NN Training Algorithm

The NN-based controller is implemented as a MultiLayer Perceptron (MLP) regressor, whose high-level implementation is shown in Fig. 1. Given the inputs of the NN, one might assume that the signal e is in principle not necessary as it can be directly derived from \hat{x} , v_{in} and \hat{i}_{out} . However, it facilitates the NN training process, further improving the model convergence and the final performances.

In contrast to traditional supervised training approaches relying on static datasets, we perform online training as the system evolution according to (2). Specifically, we apply uniformly distributed load and line step changes to the system. The $D_{c,k}^*$ is thus computed in real time via the optimization method defined in Sec. III-A. Its value is stored in a replay memory buffer, from which mini-batches were periodically sampled to update the network. In order to ensure robustness in the training phase, a probabilistic control strategy is adopted during simulation. In each time step, the $D_{c,k}$ value defining the system evolution is chosen randomly between $D_{c,k}^*$ and the one predicted by the NN. This approach ensures that the NN would be exposed to realistic trajectories, thereby improving its generalization capability and stability. The complete algorithm is provided in pseudocode form in the Algorithm 1, offering a detailed step-by-step overview of the training procedure.

IV. RESULTS VALIDATION

In order to validate the effectiveness of the proposed learning strategy, we conducted circuitual simulations. These allows to verify the NN capability of acting as a control policy for the Buck converter.

Algorithm 1 Online Training of the NN-based Controller

```

1: Initialize neural network  $\mathcal{N}_\theta$ 
2: Initialize replay memory  $\mathcal{M} \leftarrow \emptyset$ 
3: for Episode = 1 to N do
4:   Sample a random step change in  $i_{\text{out}}$  and  $v_{\text{in}}$ 
5:   for t = 1 to T do
6:     Define the vector  $\xi = [\hat{x}, \hat{i}_{\text{out}}, v_{\text{in}}, e]$ 
7:     if Rand(0, 1) <  $\epsilon$  then
8:       Compute  $D_{c,k}^*$  via projected gradient descent
9:       Store  $(\xi, D_{c,k}^*)$  in replay memory  $\mathcal{M}$ 
10:      Apply  $D_{c,k}^*$  to evolve the system
11:     else
12:       Compute duty cycle  $D_{c,k} = \mathcal{N}_\theta(x)$ 
13:       Apply  $D_{c,k}$  to evolve the system
14:     end if
15:   end for
16:   Sample a batch  $\{(\xi_i, D_{c,k_i}^*)\}$  of dimension B from  $\mathcal{M}$ 
17:   Compute the Loss:  $L = \frac{1}{B} \sum_{i=1}^B (\mathcal{N}_\theta(\xi_i) - D_{c,k_i}^*)^2$ 
18:   Update network parameters  $\theta$  using gradient descent
19: end for
    
```

TABLE II
BUCK CONVERTER AND TYPE-III CONTROLLER PARAMETERS

DC-DC Buck Converter Parameters							
L [μH]	C [μF]	R_C [m Ω]	f_{sw} [MHz]	v_{in} [V]	i_{out} [A]	R_L [Ω]	$V_{\text{out}}^{\text{target}}$ [V]
8.2	260	20	1	[6, 25]	[-0.5, 3]	5	5
Type-III Controller							
V_{ref} [mV]	$R_{c,1}$ [k Ω]	$R_{c,2}$ [k Ω]	$R_{c,3}$ [Ω]	$R_{c,4}$ [k Ω]	$C_{c,1}$ [nF]	$C_{c,2}$ [nF]	$C_{c,3}$ [pF]
800	13.3	6.65	180	2.49	5.6	1.8	150

The NN has been implemented and trained as outlined in Sec. III. Its architecture consists of a set of fully connected layers with dimensions [5, 10, 10, 1] and employs a LeakyReLU activation function with a negative slope equal to 0.01. The model is trained using the AdamW optimizer with a learning rate of 0.01, a batch size $B=64$, and a replay memory of size 512. A gradient clipping is applied with a threshold of 0.1. Referring to the Algorithm 1, an exploration probability ϵ of 0.7 is used. A total number of episodes $N=3000$ is used, with each episode evolving the system for T equal 200 steps. Input data is normalized through manual scaling by a factor of 10. The NN output is clipped between 0 and 1 after the training process, ensuring that the constraint in (3) is satisfied. This post-processing step is applied only during inference and does not affect the training process.

The performances of the proposed NN-controlled Buck converter are compared with the Voltage Mode Control (VMC) architecture [18]. The VMC architecture is readily derived by replacing the NN-based controller in Fig. 1 with a type-III compensation network, whose typical implementation is shown in Fig. 3. Its input-output

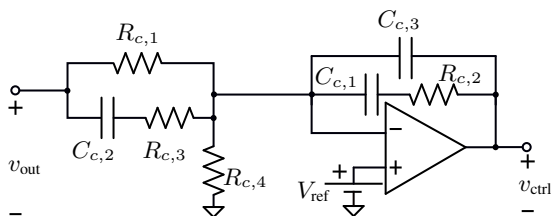


Fig. 3. Traditional Op-Amp based type-III compensation network.

transfer function in the Laplace domain is

$$G_c(s) = \frac{v_{\text{ctrl}}(s)}{v_{\text{out}}(s)} = \frac{G_{c,0} (1 + s/\omega_{z,0})(1 + s/\omega_{z,1})}{s (1 + s/\omega_{p,0})(1 + s/\omega_{p,1})}, \quad (5)$$

where $G_{c,0} = (R_{c,1}(C_{c,1} + C_{c,3}))^{-1}$, $\omega_{z,0} = (R_{c,2}(C_{c,1} + C_{c,3}))^{-1}$, $\omega_{z,1} = (C_{c,2}(R_{c,1} + R_{c,3}))^{-1}$, $\omega_{p,0} = (R_{c,3}C_{c,2})^{-1}$ and $\omega_{p,1} = (R_{c,1}(C_{c,3}||C_{c,1}))^{-1}$. The network is designed exploiting DC-DC converter averaged small-signal models in order to meet stability and dynamic performances specifications [14], [18]. Typically, the zeroes $s = -\omega_{z,\{0,1\}}$ are placed near the resonant frequency of the converter output filter, while the poles $s = -\omega_{p,\{0,1\}}$ serve to both attenuate the switching noise and cancel out the zero of the output filter induced by the presence of a non-zero R_C [19]. The gain $G_{c,0}$ is tuned to guarantee adequate stability margin and satisfactory disturbances rejection performances. For sake of space, we directly list the component values of the compensation network in Table II. These have been selected according to the DC-DC converter parameter values listed in Table II. To further mitigate the propagation of line disturbances on the output voltage, an input voltage Feed-Forward (FF) mechanism is typically implemented [20]. In practice, it consists in making the amplitude of the sawtooth waveform proportional to the converter input voltage, i.e., $V_{\text{pk}} = v_{\text{in}}/k_{\text{FF}}$, where k_{FF} is the gain of the FF stage. In the following we set $k_{\text{FF}} = 30$.

In Fig. 4, we show the system response to external disturbances when the NN-based controller and the VMC technique implementing the input voltage FF are considered. According to Fig. 4(a), the NN-based controller achieves a significantly faster settling time compared to the traditional compensator when an i_{out} step is applied. Indeed, the signal $e(t)$ stabilizes with reduced residual oscillations. In Fig. 4(b), the response of the Buck converter when an v_{in} disturbance is applied is shown. The effectiveness of the NN-based controller in minimizing the effect of the external disturbances on the converter output voltage is confirmed.

In order to further corroborate the proposed training technique, we provide a comparison between the transient response of the NN-based controller and the one obtained by directly applying the $D_{c,k}^*$ values computed as described in Sec. III-A. The results are presented in Fig. 5, showing that the NN-based controller effectively approximate the optimal $D_{c,k}^*$, achieving comparable dynamic performances.

V. CONCLUSION

This paper presents a neural network-based control strategy for a DC-DC Buck converter. The network is implemented as a tiny multilayer perceptron and it is trained online via supervised learning. The network learns to approximate the optimal control action that minimizes output voltage error when external disturbances are applied. Simulation results highlight the superior performance of the NN-based controller compared to a traditional type-III compensation network. These advantages stem from the capacity of the neural network-based controller to generalize across different operating conditions, learning an effective control policy from dynamic interactions with the system.

VI. ACKNOWLEDGMENTS

This work was partially supported by project SERICS (PE00000014) under the MUR National Recovery and Resilience Plan funded by the European Union - NextGenerationEU, and also by the FAIR - Future Artificial Intelligence Research and received funding from the European Union Next-Generation EU (Piano Nazionale di Ripresa e Resilienza (PNRR) – Missione 4 Componente 2, Investimento 1.3 – D.D. 1555 11/10/2022, PE00000013). This manuscript reflects only the authors' views and

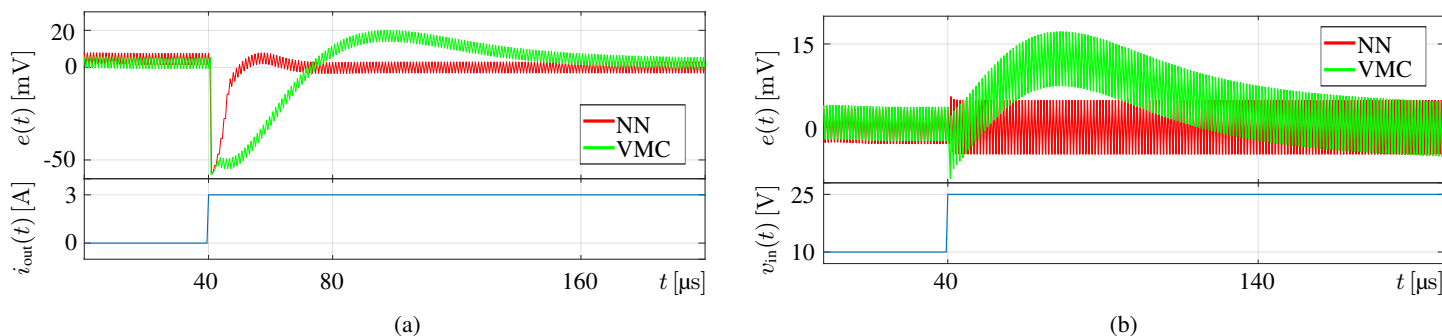


Fig. 4. Load and line transient response of the DC-DC Buck converter. We compare the proposed NN-based controller performances (NN curves) with the ones offered by the conventional VMC embedding the type-III compensation network in Fig. 3 and implementing the input voltage feed-forwarding mechanism (VMC curve). In (a) a i_{out} step disturbance is applied. In (b) a v_{in} step disturbance is applied.

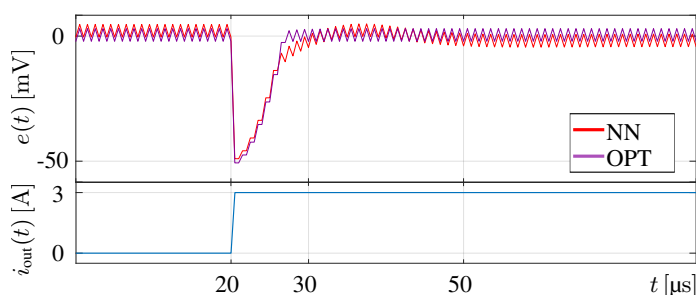


Fig. 5. Transient response of the DC-DC Buck converter. We compare the load-transient response of the converter when the proposed NN-based controller is adopted (NN curve) and the sequence of the $D_{c,k}^*$ values are applied (OPT curve).

opinions, neither the European Union nor the European Commission can be considered responsible for them.

REFERENCES

- [1] X. Yu and Y. Xue, "Smart grids: A cyber-physical systems perspective," *Proceedings of the IEEE*, vol. 104, no. 5, pp. 1058–1070, 2016. doi: 10.1109/JPROC.2015.2503119
- [2] S. K. Mazumder, A. Kulkarni, S. Sahoo, F. Blaabjerg, H. A. Mantooth, J. C. Balda, Y. Zhao, J. A. Ramos-Ruiz, P. N. Enjeti, P. R. Kumar, L. Xie, J. H. Enslin, B. Ozpineci, A. Annaswamy, H. L. Ginn, F. Qiu, J. Liu, B. Smida, C. Ogilvie, J. Ospina, C. Konstantinou, M. Stanovich, K. Schoder, M. Steurer, T. Vu, L. He, and E. P. de la Fuente, "A review of current research trends in power-electronic innovations in cyber-physical systems," *IEEE Journal of Emerging and Selected Topics in Power Electronics*, vol. 9, no. 5, pp. 5146–5163, 2021. doi: 10.1109/JESTPE.2021.3051876
- [3] M. S. Rahman, M. A. Mahmud, A. M. T. Oo, and H. R. Pota, "Multi-agent approach for enhancing security of protection schemes in cyber-physical energy systems," *IEEE Transactions on Industrial Informatics*, vol. 13, no. 2, pp. 436–447, 2017. doi: 10.1109/TII.2016.2612645
- [4] A. Humayed, J. Lin, F. Li, and B. Luo, "Cyber-physical systems security—a survey," *IEEE Internet of Things Journal*, no. 6, pp. 1802–1831, 2017. doi: 10.1109/JIOT.2017.2703172
- [5] M. B. Kamal, G. J. Mendis, and J. Wei, "Intelligent soft computing-based security control for energy management architecture of hybrid emergency power system for more-electric aircrafts," *IEEE Journal of Selected Topics in Signal Processing*, vol. 12, no. 4, pp. 806–816, 2018. doi: 10.1109/JSTSP.2018.2848624
- [6] M. R. Habibi, J. M. Guerrero, and J. C. Vasquez., "Artificial intelligence for cybersecurity monitoring of cyber-physical power electronic converters: a dc/dc power converter case study," *Scientific Reports 14, fasc. 1 (27 settembre 2024): 22072.*, 2024. doi: 10.1038/s41598-024-72286-2.
- [7] J. Chen, Y. Chen, L. Tong, L. Peng, and Y. Kang, "A backpropagation neural network-based explicit model predictive control for dc-dc converters with high switching frequency," *IEEE Journal of Emerging and Selected Topics in Power Electronics*, vol. 8, no. 3, pp. 2124–2142, 2020. doi: 10.1109/JESTPE.2020.2968475
- [8] W. Dong, S. Li, X. Fu, Z. Li, M. Fairbank, and Y. Gao, "Control of a buck dc/dc converter using approximate dynamic programming and artificial neural networks," *IEEE Transactions on Circuits and Systems I: Regular Papers*, vol. 68, no. 4, pp. 1760–1768, 2021. doi: 10.1109/TCSI.2021.3053468
- [9] C. Cui, T. Yang, Y. Dai, C. Zhang, and Q. Xu, "Implementation of transferring reinforcement learning for dc-dc buck converter control via duty ratio mapping," *IEEE Transactions on Industrial Electronics*, vol. 70, no. 6, pp. 6141–6150, 2023. doi: 10.1109/TIE.2022.3192676
- [10] M. Gheisamejad, H. Farsizadeh, and M. H. Khooban, "A novel nonlinear deep reinforcement learning controller for dc-dc power buck converters," *IEEE Transactions on Industrial Electronics*, vol. 68, no. 8, pp. 6849–6858, 2021. doi: 10.1109/TIE.2020.3005071
- [11] V. S. P. Machina, S. S. Koduru, S. Madichetty, S. Mishra, and A. E. Kamel, "Sensor attack detection and mitigation using hybrid physics informed neural networks - a real-time implementation for dc-dc converter," *IEEE Transactions on Industry Applications*, vol. 60, no. 4, pp. 5702–5713, 2024. doi: 10.1109/TIA.2024.3383806
- [12] V. S. P. Machina, S. S. Koduru, S. Madichetty, and S. Mishra, "Design of ann based controller for cyberattack detection in dc-dc buck converter," in *2022 22nd National Power Systems Conference (NPSC)*, 2022, pp. 460–464. doi: 10.1109/NPSC57038.2022.10068889
- [13] M. T. Lê, P. Wolinski, and J. Arbel, "Efficient neural networks for tiny machine learning: A comprehensive review," 2023. [Online]. Available: <https://arxiv.org/abs/2311.11883>
- [14] R. W. Erickson and D. Maksimovic, *Fundamentals of Power Electronics*, 3rd ed. Springer International Publishing, 2020.
- [15] C.-C. Fang, "Sampled-data poles, zeros, and modeling for current-mode control," *International Journal of Circuit Theory and Applications*, vol. 41, no. 2, pp. 111–127, 2013. doi: 10.1002/cta.790
- [16] S. K. Pandey, S. L. Patil, U. M. Chaskar, and S. B. Phadke, "State and disturbance observer-based integral sliding mode controlled boost dc-dc converters," *IEEE Transactions on Circuits and Systems II: Express Briefs*, vol. 66, no. 9, pp. 1567–1571, 2019. doi: 10.1109/TC-SII.2018.2888570
- [17] S. Zhuo, A. Gaillard, L. Xu, D. Paire, and F. Gao, "Extended state observer-based control of dc-dc converters for fuel cell application," *IEEE Transactions on Power Electronics*, vol. 35, no. 9, pp. 9923–9932, 2020. doi: 10.1109/TPEL.2020.2974556
- [18] D. Meeks, "Loop stability analysis of voltage mode buck regulator," Texas Instruments, Tech. Rep. SLVA301, 2008, application Report. [Online]. Available: <https://www.ti.com/lit/an/slva301/slva301.pdf>
- [19] H. Sahoo, S. Kapat, and B. Singh, "Small-signal modelling and analysis of converter interactivity in low-voltage dc grid," in *2021 IEEE 6th International Conference on Computing, Communication and Automation (ICCCA)*, 2021, pp. 708–713. doi: 10.1109/ICCCA52192.2021.9666397
- [20] M. Kazimierzczuk and A. Edstrom, "Open-loop peak voltage feedforward control of pwm buck converter," *IEEE Transactions on Circuits and Systems I: Fundamental Theory and Applications*, vol. 47, no. 5, pp. 740–746, 2000. doi: 10.1109/81.847879